

Electronic Supplementary Information (ESI) for

Porosity regulation of metal-organic frameworks for high proton conductivity by rational ligand design: mono- versus disulfonyl-4,4'-biphenyldicarboxylic acid

Shunlin Zhang,^a Yuxin Xie,^a Mengrui Yang,^a Dunru Zhu^{ab*}

^a College of Chemical Engineering, State Key Laboratory of Materials-oriented Chemical Engineering, Nanjing Tech University, 30 Puzhu South Road, Nanjing, Jiangsu 211816, China.

^b State Key Laboratory of Coordination Chemistry, Nanjing University, 163 Xianlin Avenue, Nanjing, Jiangsu 210023, China.

*Correspondence e-mail: zhudr@njtech.edu.cn

Contents

1. The FT-IR and ¹ HNMR spectra of H₃L	S2
2. Molecular structures of MOFs 1-3	S3
3. The FT-IR spectra of MOFs 1-3	S4
4. The PXRD patterns of MOFs 1-3	S5
5. The thermogravimetric analysis of MOFs 1-3	S7
6. Crystal structure determination.....	S8
7. Proton conductivity measurement.....	S10

1. The FT-IR and ¹HNMR spectra of H₃L

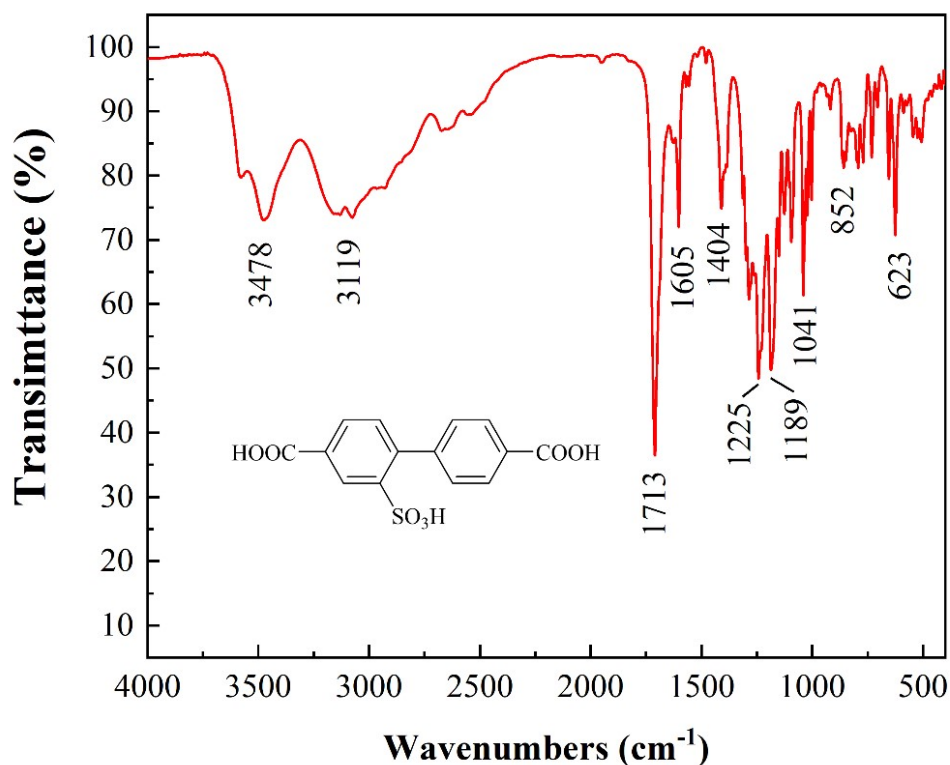


Fig. S1 FT-IR spectra of H₃L.

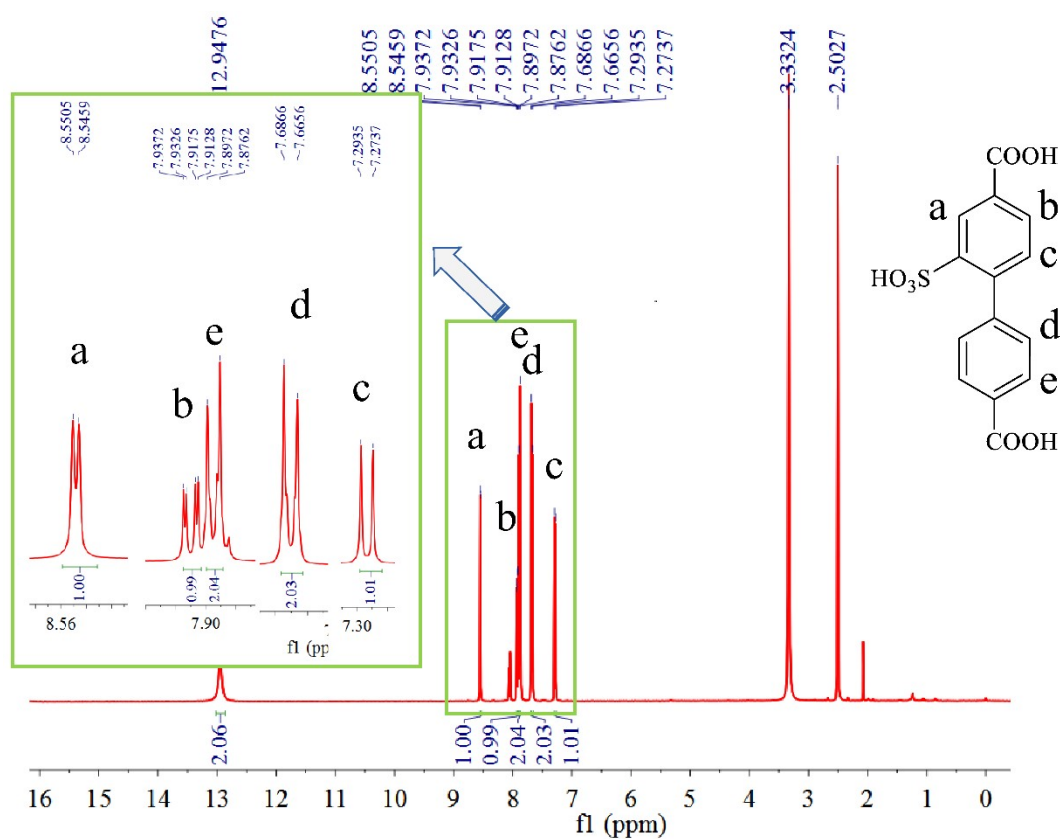


Fig. S2 ¹HNMR spectrum of H₃L

2. Molecular structures of MOFs 1-3

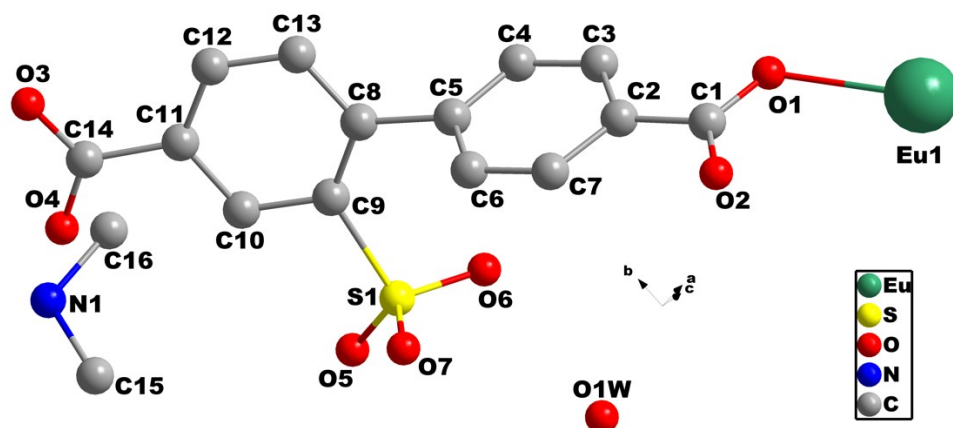


Fig. S3 Asymmetric unit of **1** (H and disordered atoms are omitted for clarity).

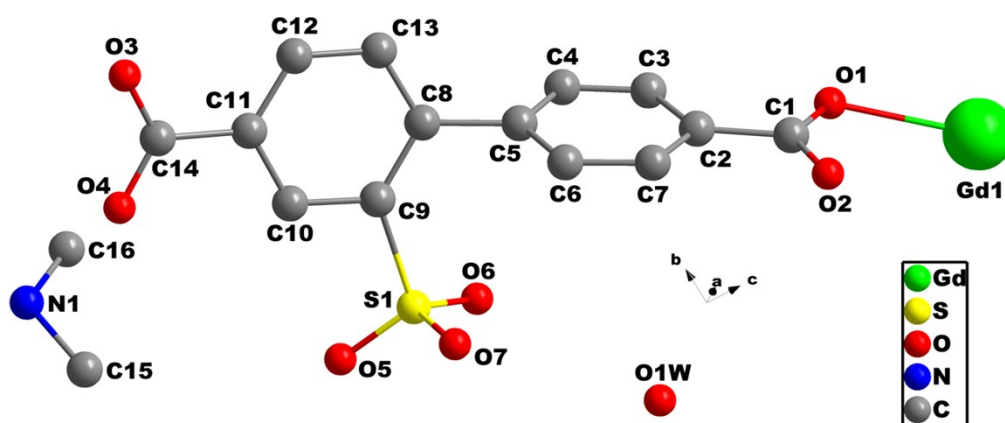


Fig. S4 Asymmetric unit of **2** (H and disordered atoms are omitted for clarity).

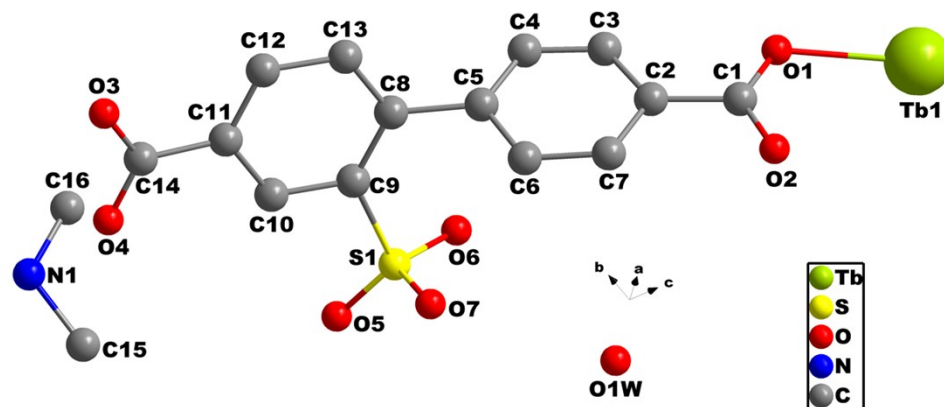


Fig. S5 Asymmetric unit of **3** (H and disordered atoms are omitted for clarity).

3. The FT-IR spectra of MOFs 1-3

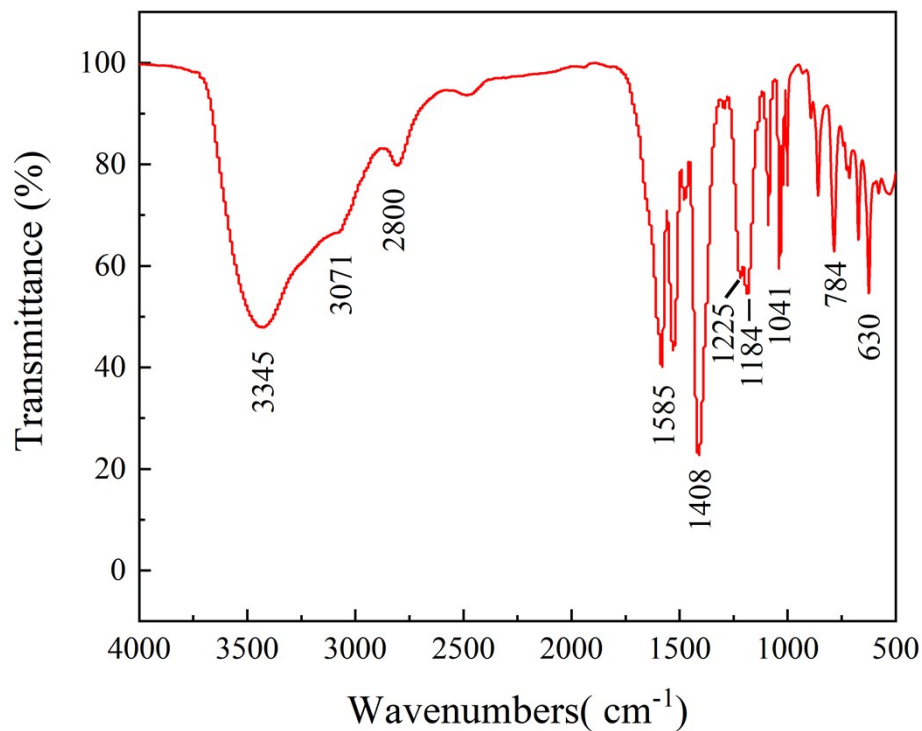


Fig. S6 FT-IR spectra of 1.

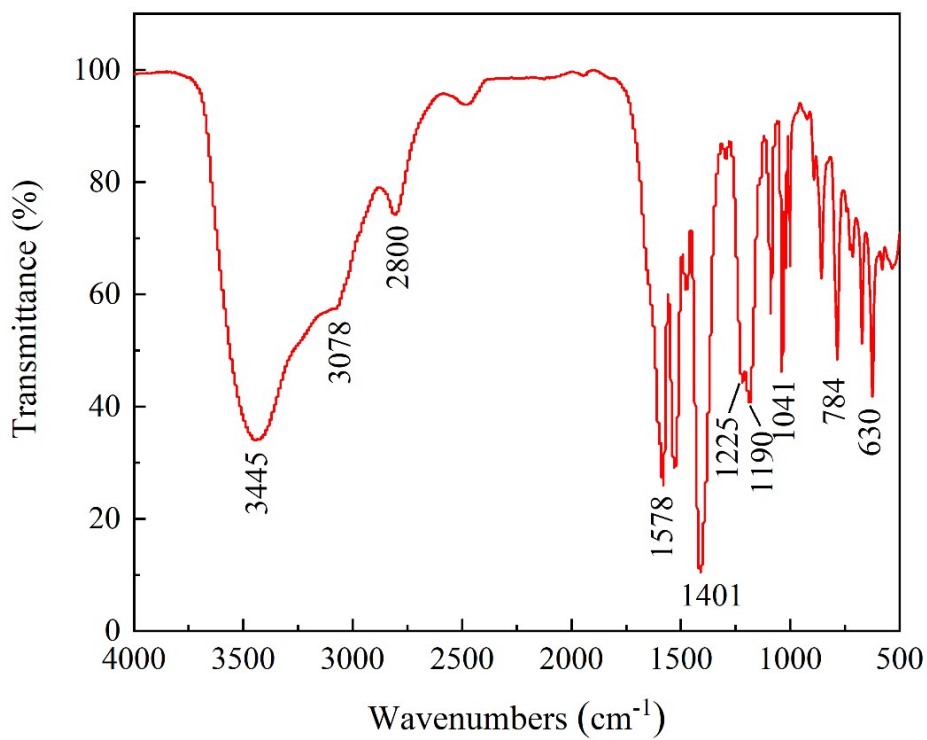


Fig. S7 FT-IR spectra of 2.

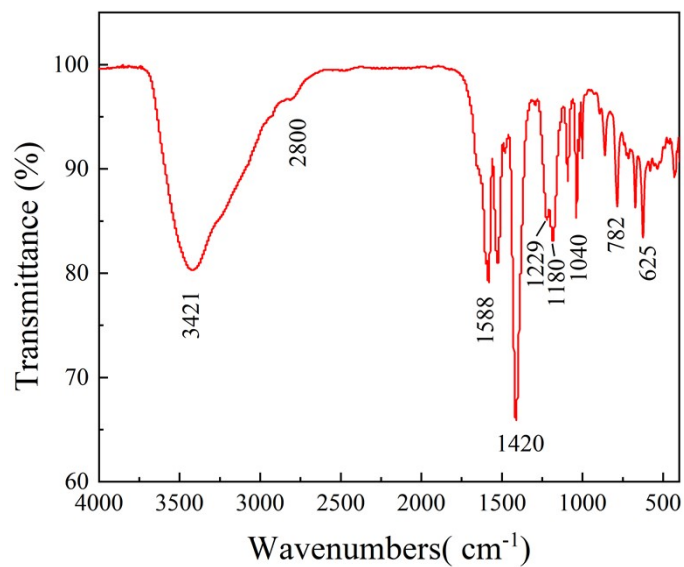


Fig. S8 FT-IR spectra of **3**.

4. The PXRD patterns of MOFs 1-3

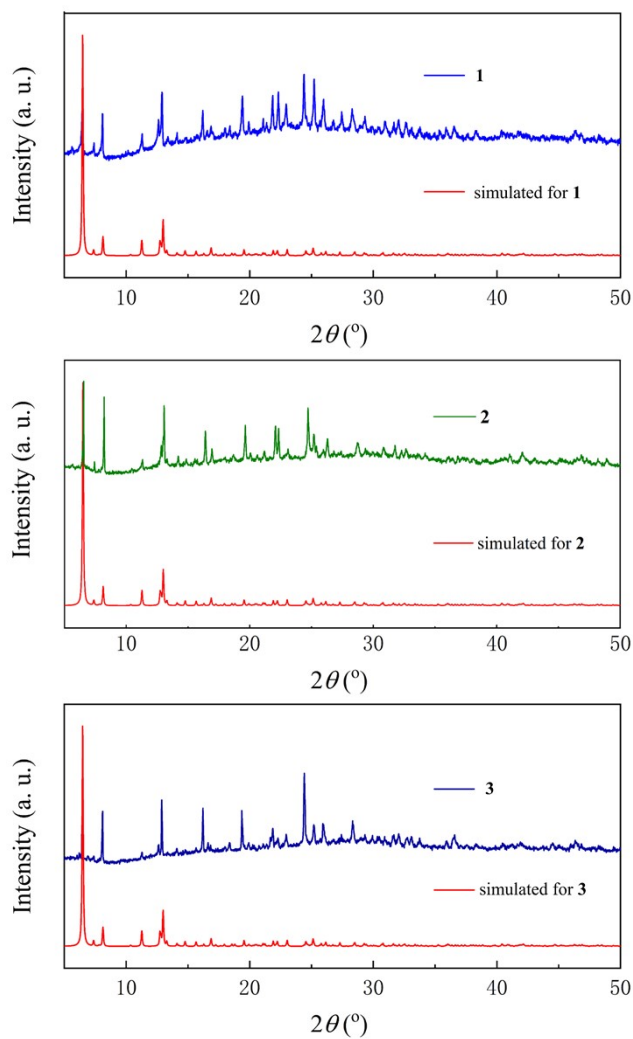


Fig. S9 Experimental and simulated powder X-ray diffraction patterns of MOFs **1-3**.

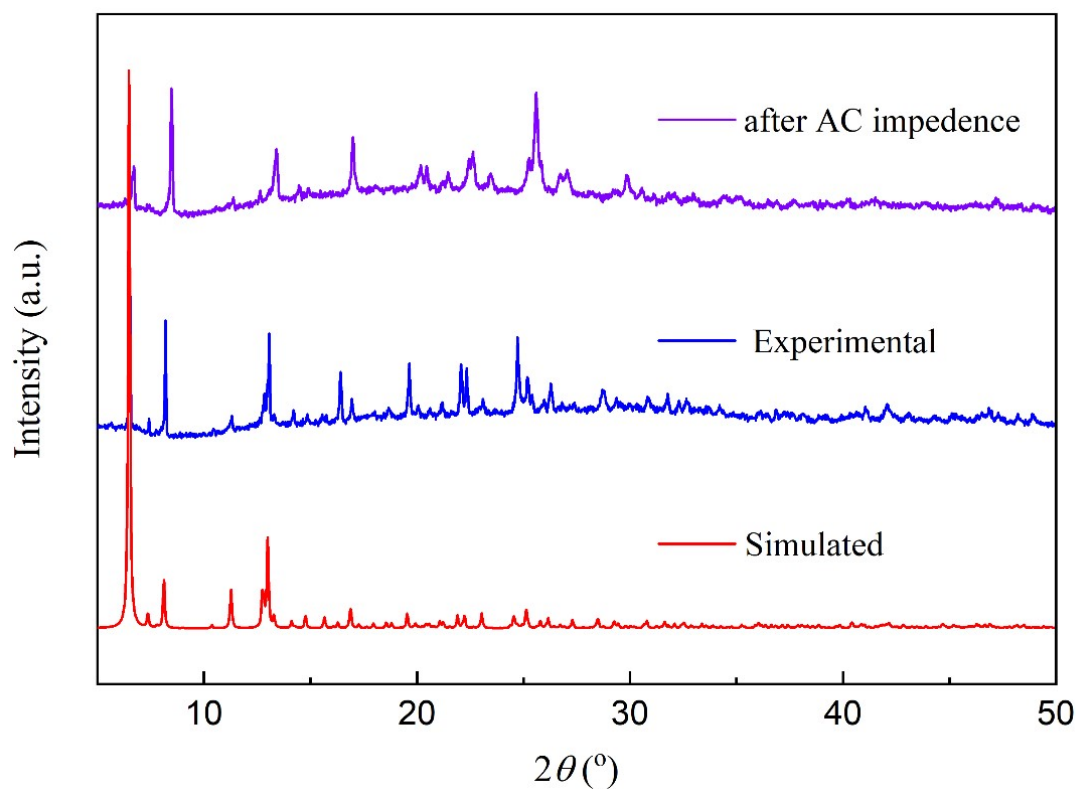


Fig. S10 Experimental and simulated PXRd patterns of **2** and after 72h AC impedance measurements.

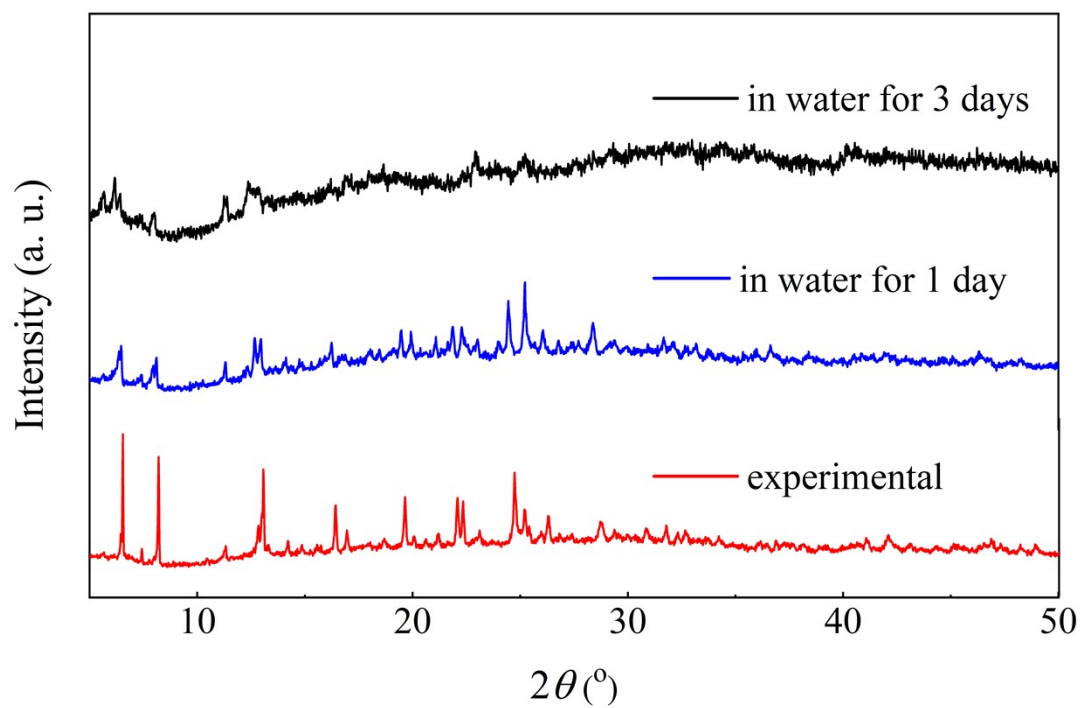


Fig. S11 Experimental PXRd patterns of **2** and after water immersion.

5. The thermogravimetric analysis of MOFs 1-3

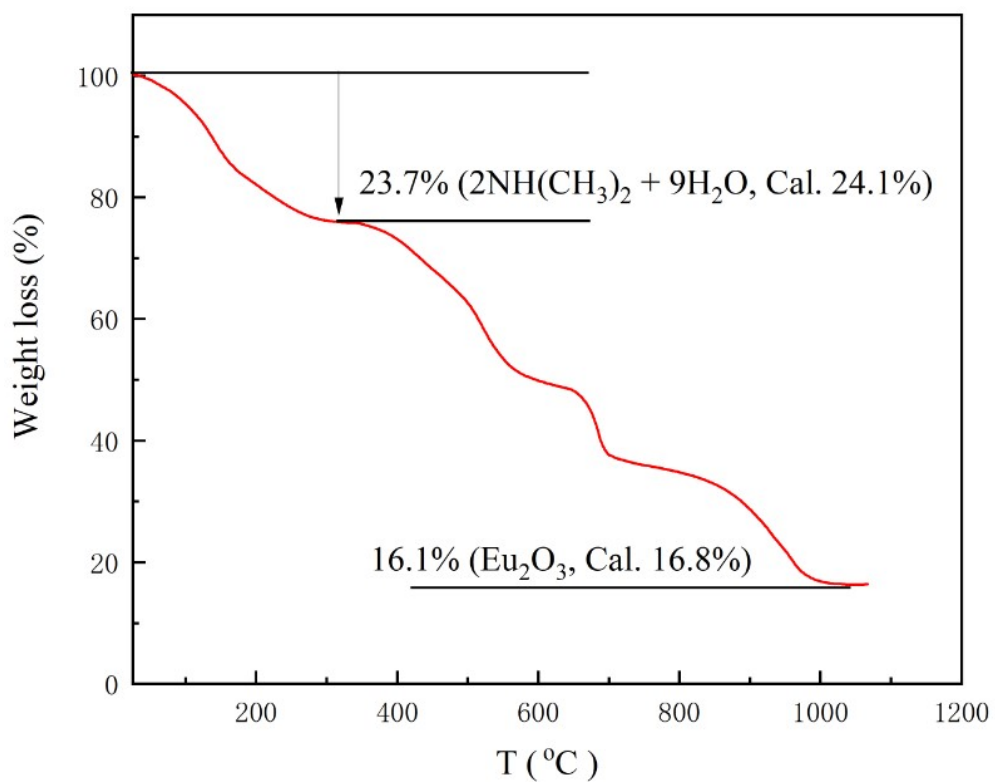


Fig. S12 TGA curve for **1**

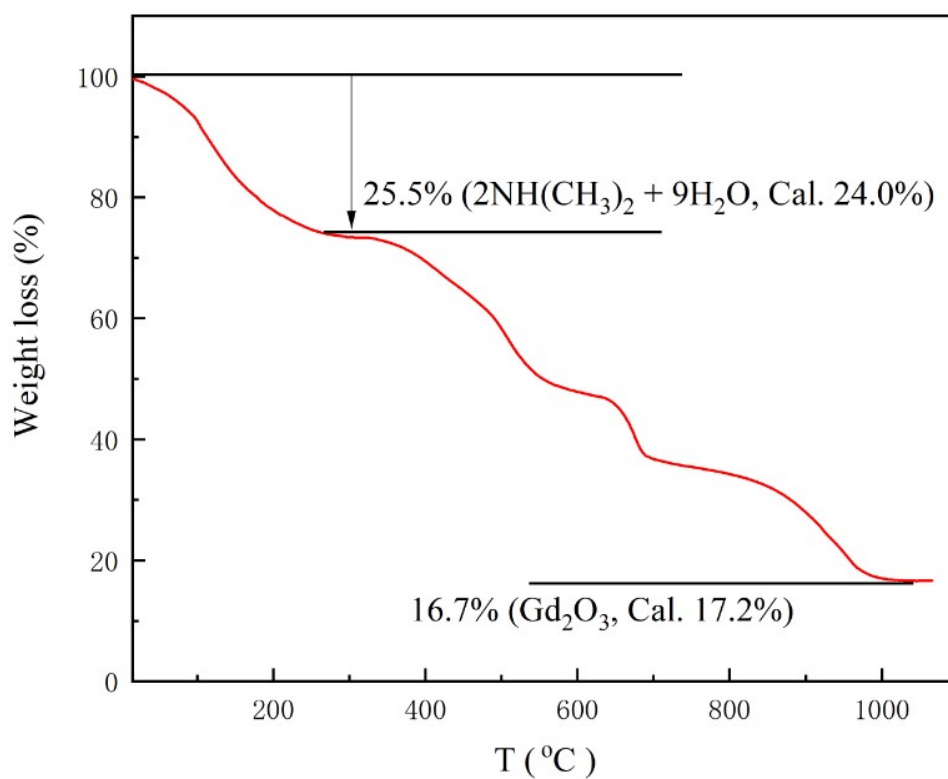


Fig. S13 TGA curve for **2**

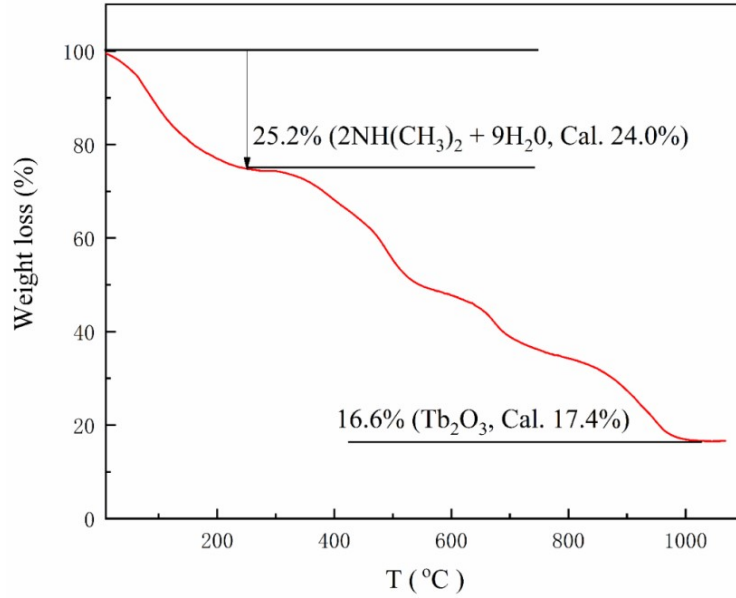


Fig. S14 TGA curve for **3**

6. Crystal structure determination

Table S1 Crystallographic data for **MOFs 1-3**

MOFs	1	2	3
Empirical formula	$C_{32}H_{49}EuN_2O_{23}S_2$	$C_{32}H_{49}GdN_2O_{23}S_2$	$C_{32}H_{49}TbN_2O_{23}S_2$
Formula weight	1045.83	1051.11	1052.79
Crystal system	Orthorhombic	Orthorhombic	Orthorhombic
Space group	<i>Pnnn</i>	<i>Pnnn</i>	<i>Pnnn</i>
<i>a</i> (Å)	14.1253(17)	14.1306(15)	14.1106(8)
<i>b</i> (Å)	17.038(2)	17.0415(18)	17.1352(9)
<i>c</i> (Å)	22.649(3)	22.636(2)	22.4486(12)
<i>V</i> (Å ³)	5450.9(12)	5450.9(10)	5427.8(5)
<i>Z</i>	4	4	4
<i>D_c</i> (g·cm ⁻³)	1.096	1.103	1.109
μ (mm ⁻¹)	1.275	1.341	1.428
<i>F</i> (000)	1808.0	1812.0	1816.0
Crystal size (mm ³)	0.25×0.15×0.10	0.25×0.13×0.10	0.25×0.13×0.10
θ Range (°)	1.496-24.998	1.496-24.998	1.495-25.048
Reflections collected	36995	36891	36784
Independent reflections	4826 [<i>R</i> _{int} = 0.044]	4826 [<i>R</i> _{int} = 0.0268]	4825 [<i>R</i> _{int} = 0.0407]
Reflections observed [<i>I</i> > 2σ(<i>I</i>)]	3087	3331	3064
Data/restraints/parameters	4826/360/321	4826/216/323	4825/372/321
Goodness-of-fit on <i>F</i> ²	1.090	1.082	1.099
<i>R</i> ₁ / <i>wR</i> ₂ [<i>I</i> > 2σ(<i>I</i>)]	0.0624/0.2249	0.0597/0.2134	0.0629/0.2261
<i>R</i> ₁ / <i>wR</i> ₂ (all data)	0.0889/0.2503	0.0783/0.2381	0.0905/0.2502
Max., Min. Δρ (e·Å ⁻³)	1.325, -0.906	2.156, -0.820	2.001, -0.866

Table S2 Selected bond lengths (Å) and angles (°) for **1-3**

1			
Eu1–O1	2.414(5)	Eu1–O3 ⁱ	2.477(6)
Eu1–O2 ⁱⁱ	2.313(5)	Eu1–O4 ⁱ	2.487(5)
2			
Gd1–O1	2.413(4)	Gd1–O3 ⁱ	2.468(5)
Gd1–O2 ⁱⁱ	2.311(4)	Gd1–O4 ⁱ	2.485(4)
3			
Tb1–O1	2.373(5)	Tb1–O3 ⁱ	2.455(5)
Tb1–O2 ⁱⁱ	2.289(5)	Tb1–O4 ⁱ	2.458(5)
1			
O2–Eu1–O2 ⁱⁱ	107.2(3)	O3 ⁱ –Eu1–O3 ^{iv}	95.0(3)
O2–Eu1–O1	80.70(18)	O2–Eu1–O4 ⁱ	156.86(18)
O2 ⁱⁱ –Eu1–O1	81.03(19)	O2 ⁱⁱ –Eu1–O4 ⁱ	78.71(18)
O2–Eu1–O1 ⁱⁱⁱ	81.03(19)	O1–Eu1–O4 ⁱ	78.14(17)
O2 ⁱⁱ –Eu1–O1 ⁱⁱⁱ	80.70(18)	O1 ⁱⁱⁱ –Eu1–O4 ⁱ	122.10(17)
O1–Eu1–O1 ⁱⁱⁱ	149.0(2)	O3 ⁱ –Eu1–O4 ⁱ	52.45(17)
O2–Eu1–O3 ⁱ	147.94(18)	O3 ^{iv} –Eu1–O4 ⁱ	77.61(18)
O2 ⁱⁱ –Eu1–O3 ⁱ	87.42(19)	O2–Eu1–O4 ^{iv}	78.71(18)
O1–Eu1–O3 ⁱ	130.58(18)	O2 ⁱⁱ –Eu1–O4 ^{iv}	156.86(18)
O1 ⁱⁱⁱ –Eu1–O3 ⁱ	73.20(19)	O1–Eu1–O4 ^{iv}	122.10(17)
O2–Eu1–O3 ^{iv}	87.42(19)	O1 ⁱⁱⁱ –Eu1–O4 ^{iv}	78.14(17)
O2 ⁱⁱ –Eu1–O3 ^{iv}	147.94(18)	O3 ⁱ –Eu1–O4 ^{iv}	77.61(18)
O1–Eu1–O3 ^{iv}	73.20(19)	O3 ^{iv} –Eu1–O4 ^{iv}	52.45(17)
O1 ⁱⁱⁱ –Eu1–O3 ^{iv}	130.58(18)	O4 ⁱ –Eu1–O4 ^{iv}	104.9(2)
2			
O2–Gd1–O2 ⁱⁱ	106.7(2)	O3 ⁱ –Gd1–O3 ^{iv}	95.2(3)
O2–Gd1–O1	81.13(16)	O2–Gd1–O4 ⁱ	156.78(15)
O2 ⁱⁱ –Gd1–O1	81.13(16)	O2 ⁱⁱ –Gd1–O4 ⁱ	79.03(15)
O2–Gd1–O1 ⁱⁱⁱ	81.13(16)	O1–Gd1–O4 ⁱ	78.14(14)
O2 ⁱⁱ –Gd1–O1 ⁱⁱⁱ	80.57(15)	O1 ⁱⁱⁱ –Gd1–O4 ⁱ	122.08(14)
O1–Gd1–O1 ⁱⁱⁱ	149.1(2)	O3 ⁱ –Gd1–O4 ⁱ	52.60(14)
O2–Gd1–O3 ⁱ	147.97(14)	O3 ^{iv} –Gd1–O4 ⁱ	77.49(15)
O2 ⁱⁱ –Gd1–O3 ⁱ	87.54(16)	O2–Gd1–O4 ^{iv}	79.03(15)
O1–Gd1–O3 ⁱ	130.72(15)	O2 ⁱⁱ –Gd1–O4 ^{iv}	156.78(15)
O1 ⁱⁱⁱ –Gd1–O3 ⁱ	72.98(16)	O1–Gd1–O4 ^{iv}	78.14(14)
O2–Gd1–O3 ^{iv}	87.54(16)	O1 ⁱⁱⁱ –Gd1–O4 ^{iv}	122.08(14)
O2 ⁱⁱ –Gd1–O3 ^{iv}	147.97(15)	O3 ⁱ –Gd1–O4 ^{iv}	77.49(15)
O1–Gd1–O3 ^{iv}	72.98(16)	O3 ^{iv} –Gd1–O4 ^{iv}	52.60(14)
O1 ⁱⁱⁱ –Gd1–O3 ^{iv}	130.72(14)	O4 ⁱ –Gd1–O4 ^{iv}	104.7(2)
3			
O2–Tb1–O2 ⁱⁱ	107.2(3)	O3 ⁱ –Tb1–O3 ^{iv}	94.6(3)
O2–Tb1–O1	80.12(19)	O2–Tb1–O4 ⁱ	156.19(18)

O2 ⁱⁱ -Tb1-O1	80.90(19)	O2 ⁱⁱ -Tb1-O4 ⁱ	78.49(18)
O2-Tb1-O1 ⁱⁱⁱ	80.9(2)	O1-Tb1-O4 ⁱ	77.99(18)
O2 ⁱⁱ -Tb1-O1 ⁱⁱⁱ	80.12(19)	O1 ⁱⁱⁱ -Tb1-O4 ⁱ	122.88(18)
O1-Tb1-O1 ⁱⁱⁱ	147.7(3)	O3 ⁱ -Tb1-O4 ⁱ	52.82(18)
O2-Tb1-O3 ⁱ	148.32(18)	O3 ^{iv} -Tb1-O4 ⁱ	77.71(18)
O2 ⁱⁱ -Tb1-O3 ⁱ	87.36(19)	O2-Tb1-O4 ^{iv}	78.49(18)
O1-Tb1-O3 ⁱ	130.79(18)	O2 ⁱⁱ -Tb1-O4 ^{iv}	156.19(18)
O1 ⁱⁱⁱ -Tb1-O3 ⁱ	73.94(19)	O1-Tb1-O4 ^{iv}	122.88(18)
O2-Tb1-O3 ^{iv}	87.36(19)	O1 ⁱⁱⁱ -Tb1-O4 ^{iv}	77.99(18)
O2 ⁱⁱ -Tb1-O3 ^{iv}	148.32(18)	O3 ⁱ -Tb1-O4 ^{iv}	77.71(18)
O1-Tb1-O3 ^{iv}	73.9(2)	O3 ^{iv} -Tb1-O4 ^{iv}	52.82(18)
O1 ⁱⁱⁱ -Tb1-O3 ^{iv}	130.79(18)	O4 ⁱ -Tb1-O4 ^{iv}	105.9(3)

Symmetry codes: (i) $1/2+x, 1-y, 1/2+z$; (ii) $1/2-x, y, 3/2-z$; (iii) $x, 1/2-y, 3/2-z$; (iv) $1/2+x, 1/2-y, 1-z$.

Table S3 Hydrogen-bonding geometry (Å, °) for **2**

D-H...A	d(D-H)	d(H...A)	d(D...A)	∠D-H...A
N1-H1A...O4	0.89	2.26	2.893(10)	128
N1-H1B...O5A ⁱ	0.89	1.85	2.604(3)	141
O1W-H1WA...O7	0.85	2.53	3.352(5)	163
O1W-H1WB...O6 ⁱⁱ	0.85	2.92	3.751(5)	169
O1W-H1WC...O7A ⁱⁱⁱ	0.85	2.96	3.734(6)	154
O1WA-H1WD...O6	0.85	2.19	3.009(2)	161
O1WA-H1WE...O5 ⁱ	0.85	2.50	3.123(4)	131
O1WA-H1WF...O1WA ^{iv}	0.85	2.39	3.230(7)	170
C15-H15C...O4	0.96	2.48	3.004(2)	115
C16-H16C...π ⁱ	0.96	2.67	3.598(3)	162
C6-H6...π ^v	0.93	3.24	3.943(2)	134

Symmetry codes: (i) $1/2-x, y, 1/2-z$; (ii) $1/2-x, 1/2-y, z$; (iii) $x-1/2, y-1/2, 1-z$; (iv) $x, 1/2-y, 1/2-z$; (v) $-x, 1-y, 1-z$.

7. Proton conductivity measurement

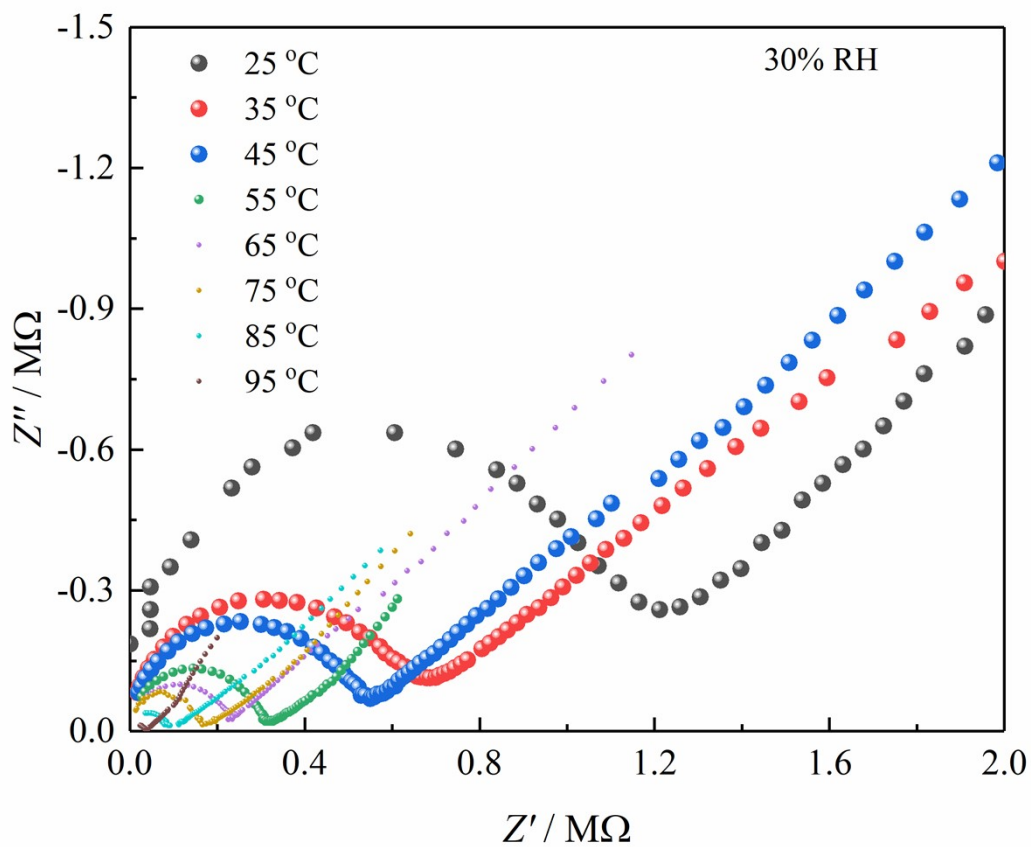


Fig. S15 Temperature-dependent Nyquist plots of **2** under 30% RH

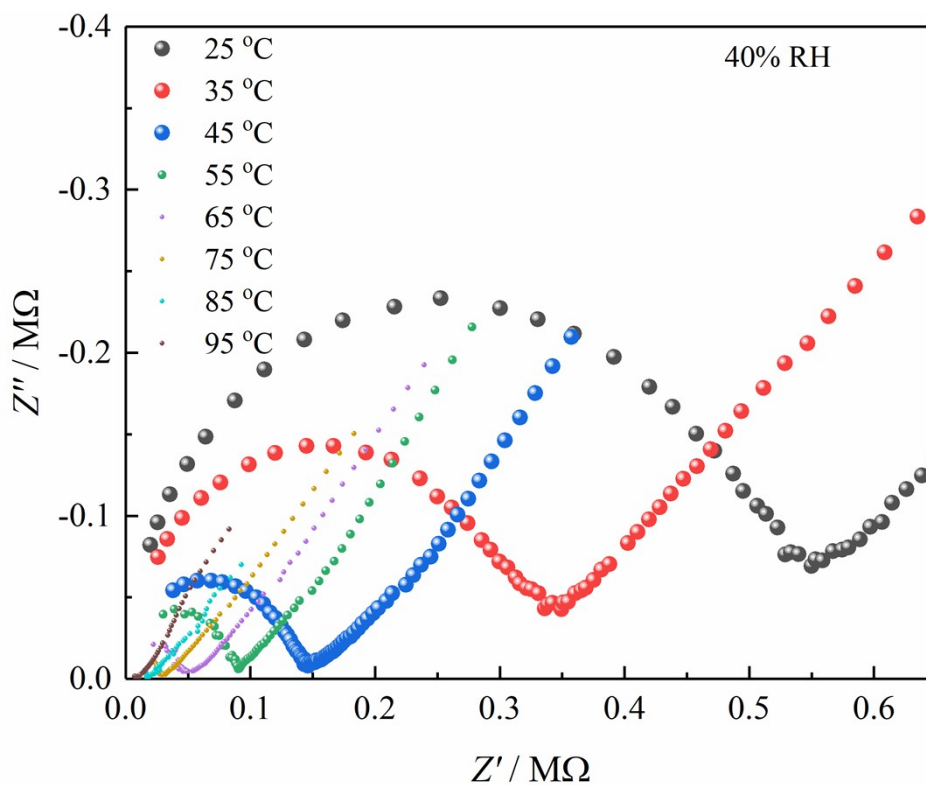


Fig. S16 Temperature-dependent Nyquist plots of **2** under 40% RH

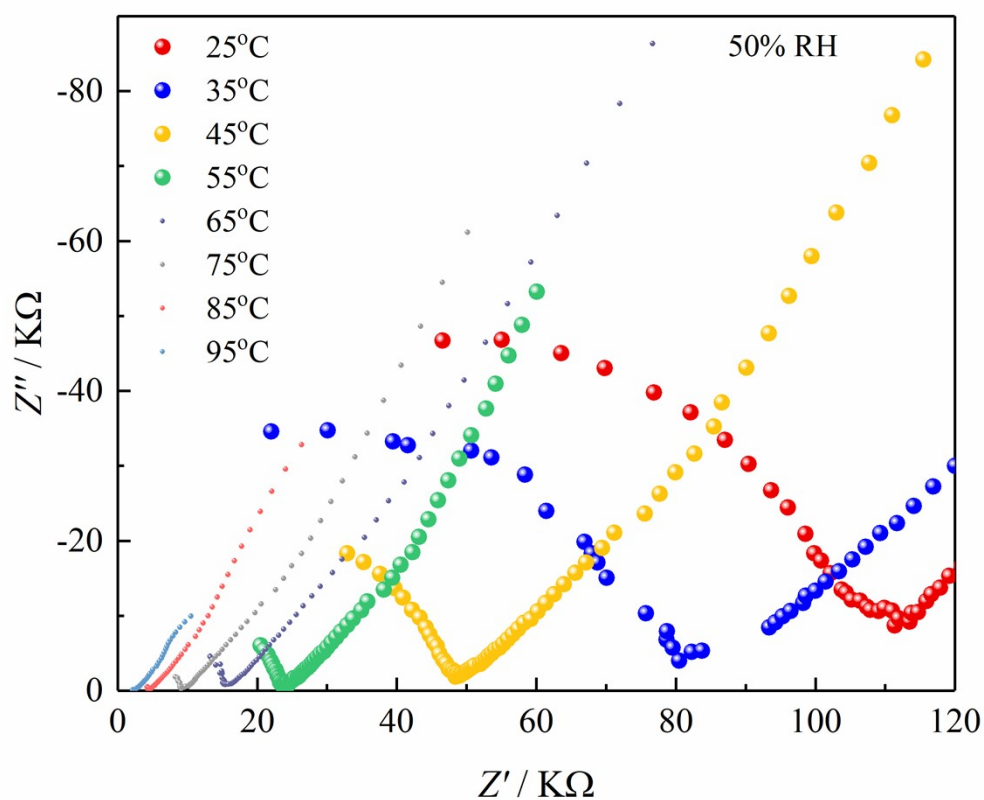


Fig. S17 Temperature-dependent Nyquist plots of **2** under 50% RH

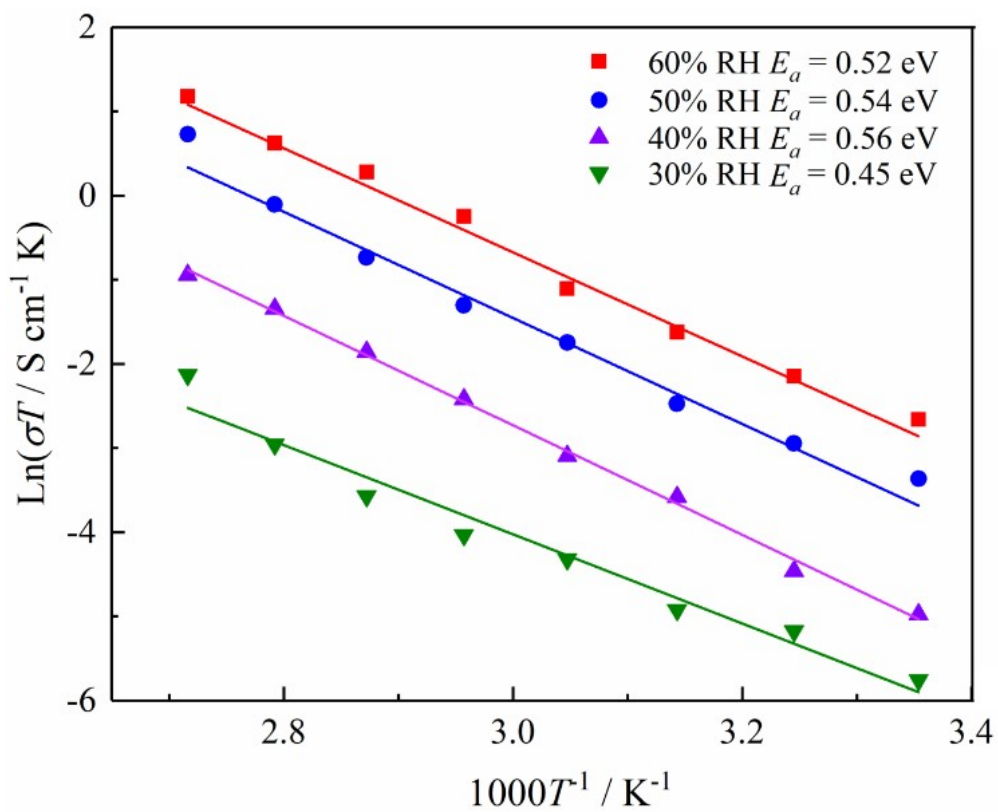


Fig. S18 Arrhenius plot of **2** at 30-60% RH

Table S4 Proton conductivities for **2** at various RH and temperature

T (°C)	σ (S cm ⁻¹)			
	30% RH	40% RH	50% RH	60% RH
25	1.06×10^{-5}	2.32×10^{-5}	1.16×10^{-4}	2.35×10^{-4}
35	1.84×10^{-5}	3.75×10^{-5}	1.70×10^{-4}	3.80×10^{-4}
45	2.28×10^{-5}	8.76×10^{-5}	2.65×10^{-4}	6.20×10^{-4}
55	4.04×10^{-5}	1.38×10^{-4}	5.32×10^{-4}	1.01×10^{-3}
65	5.23×10^{-5}	2.63×10^{-4}	8.04×10^{-4}	2.31×10^{-3}
75	8.06×10^{-5}	4.50×10^{-4}	1.38×10^{-3}	3.80×10^{-3}
85	1.45×10^{-4}	7.28×10^{-4}	2.51×10^{-3}	5.22×10^{-3}
95	3.22×10^{-4}	1.06×10^{-3}	5.62×10^{-3}	8.83×10^{-3}